Temporal Shaping of Femtosecond Solitary Pulses in Photoionized Media

Hélène Ward and Luc Bergé

Département de Physique Théorique et Appliquée, CEA-DAM/Ile de France, B.P. No. 12, F-91680 Bruyères-le-Châtel, France

(Received 3 July 2002; published 6 February 2003)

Femtosecond light pulses interacting with solids are studied. With a power close to the self-focusing threshold, an optical pulse evolves like a solitary wave with a temporal duration shrunk to a few femtoseconds through the defocusing action of multiphoton ionization. Self-steepening and space-time focusing are shown to form shock profiles, which do not prevent the pulse from keeping a shorter duration over one Rayleigh length. Theoretical estimates justify the key mechanisms leading to pulse compression, whose influence on the power spectra is finally discussed.

DOI: 10.1103/PhysRevLett.90.053901 PACS numbers: 42.65.Tg, 42.65.Jx, 42.68.Ay

The self-guiding of ultrashort laser pulses in matter has become a topic of intense research activities, stimulated by the rapid progress of femtosecond (fs) laser sources and their potential applications. For instance, laser beams with 100 fs duration and intensities limited to 10^{14} W/cm^2 form long-range filaments in the atmosphere, which opens new trends in light detection and ranging (LIDAR) techniques [1–4]. Transparent solids also produce comparable objects, promoted by the same physical processes [5]. From the Kerr response of the medium, a light pulse with input power above the critical threshold for self-focusing (SF) first focuses at a finite distance. While increasing in intensity, the light excites an electron plasma by multiphoton ionization (MPI), which partly defocuses the beam. At high enough powers, a dynamic balance between SF and MPI then maintains a light channel through several focusing/defocusing cycles, which generate multipeaked temporal profiles [1–3]. In glass, for example, experimental observation of two-peaked profiles was reported [5] at input powers equal to 5 times the critical power for SF. Such temporal distortions result from plasma generation, which depletes the back of the pulse while preserving a sharp leading peak. Upon further propagation, this peak decays, whereas the back of the pulse refocuses spatially [2]. Two peaks with comparable intensities thus emerge, and they extend over the FWHM duration of the input pulse.

At lower powers, however, the dynamic interplay between SF and MPI may be stabilized along the propagation axis. The light channel then behaves like a spatial soliton, whose temporal profile is shrunk by plasma defocusing to a single time slice [4,6]. These solitary pulses can nonetheless disappear to the benefit of shock structures created by self-steepening and space-time focusing, when the latter effects arise earlier than MPI [7].

In view of the previous studies, we can wonder whether photoionization may be "tuned" at specific optical powers to reduce significantly the pulse duration, which would have an important incidence on further technological developments of ultrafast laser sources. On the one hand, too powerful lasers produce multiple peaks in time [5], which cannot yield an effective pulse shortening. On the other hand, SF pulses with low enough power can noticeably be compressed by MPI [6], but steepening effects severely distort the resulting solitary wave through a shock dynamics [7]. The question of controlling the interplay between these two key processes for promoting shorter pulses thus remains open. To achieve this goal, the pulse profile must result in one dominant peak with a narrow extension in time, propagating over an experimentally accessible self-channeling distance.

Here we show that fs pulses can actually be shortened to few-cycle durations over the Rayleigh range, through the combined action of MPI and pulse steepening terms. To address this point, we simulate a fs pulse with power moderately above critical, and we make it propagate like an intense filament clamped with a MPI source. This filament then undergoes multiphoton absorption (MPA), self-steepening, and space-time focusing, whose incidence on the temporal pulse profiles, on the propagation range, and on spectral broadening is analyzed separately.

We consider a linearly polarized beam propagating in fused silica with central frequency ω_0, wave number $k = n_0 k_0$ ($k_0 = \omega_0/c$), and laser wavelength $\lambda_0 = 790$ nm. At the entrance face of the glass sample, the beam profile is Gaussian: $\sqrt{2P_{\rm in}/\pi w_0^2}\,\exp(-r^2/w_0^2 - t^2/t_p^2)$ with input power $P_{\rm in} = 1.5P_{\rm cr}$, beam waist $w_0 = 15\ \mu$m, and temporal FWHM diameter $\sqrt{2\ln 2}\,t_p = 160$ fs. The critical power for self-focusing is $P_{\rm cr} = \lambda_0^2/2\pi n_0 n_2 \simeq 2.2$ MW with $n_2 = 3.2 \times 10^{-16}$ cm^2/W ($n_0 = 1.4$) corresponding to the nonlinear (linear) refraction index of fused silica. Following standard models [2–6], the complex envelope $\mathcal{E}(r, t, z)$ of the electric field and the electron density ρ of the excited plasma evolve as

$$i\partial_z\mathcal{E} + \frac{1}{2k}T^{-1}\nabla_\perp^2\mathcal{E} - \frac{k''}{2}\partial_t^2\mathcal{E} + k_0 n_2 T(|\mathcal{E}|^2\mathcal{E}) - \frac{k_0}{2n_0\rho_c}T^{-1}(\rho\mathcal{E}) + i\frac{\beta^{(K)}}{2}|\mathcal{E}|^{2K-2}\mathcal{E} = 0, \quad (1)$$

$$\partial_t\rho = \sigma_K\rho_{at}|\mathcal{E}|^{2K}(1 - \rho/\rho_{at}), \qquad \rho \ll \rho_{at}, \quad (2)$$

where z is the propagation distance and t the retarded time ($t - z/v_g$) with group velocity v_g. The transverse

Laplacian describes the diffraction of axis-symmetric beams and $k'' = [\partial^2\omega/\partial k^2]^{-1}|_{\omega_0} = 340$ fs^2/cm is the group velocity dispersion (GVD) coefficient. The following terms in Eq. (1) are the Kerr response of the material, plasma defocusing promoted by MPI and MPA with coefficient $\beta^{(K)} = K\hbar\omega_0\sigma_K\rho_{at}$. The critical plasma density, ρ_c, and the background atom density, $\rho_{at} = 2.1 \times 10^{22}$ atoms/cm^3, are in the ratio $\rho_{at}/\rho_c = 11.75$. Band-to-band transitions are induced in silica from the gap potential $U_i = 7.8$ eV [6], yielding the number of photons $K = 5$ required for ionization. The MPI coefficient in Eq. (2) then reads as $\sigma_K = 1.3 \times 10^{-55}$ s^{-1} cm^{2K}/W^K. Through the operator $T \equiv 1 + (i/\omega_0)\partial_t$, we included self-steepening effects modeled by T in front of the cubic nonlinearity, and space-time focusing with T^{-1} in front of the transverse Laplacian. These operators take into account the deviations from the slowly varying envelope approximation (SVEA), which makes the model (1) and (2) valid up to the single-cycle limit [7,8]. Because MPI alone determines the mean level of free electrons created by ionization on comparable time scales [5], we neglect avalanche and recombination processes. Accordingly, plasma dissipation is discarded. Equation (1) is solved by means of a Fourier spectral decomposition in time and a standard Cranck-Nicholson scheme in space. Equation (2) is solved by a semianalytic integration [3]. Calculations were performed with high accuracy, by using grid spacings of $5 \times 10^{-3} w_0$ in r and $5 \times 10^{-4} t_p$ in time. Longitudinal steps Δz were decreased to 0.02 μm to resolve steep profiles around the nonlinear focus. So, each simulation required several hundred hours of CPU time.

To start with, we show in Figs. 1(a) and 1(b) the maximum-in-time (peak) light intensity and electron density obtained in the limit $T = 1$. With no MPA, the beam first self-focuses, then triggers an electron plasma. Arrest of collapse proceeds from plasma generation, whereas GVD remains of negligible influence. As expected for powers close to critical, SF is smoothly balanced by MPI around the threshold intensity $|\mathcal{E}|^2_{\max} \sim \rho^{\max}/2\rho_c n_0 n_2$, where $\rho^{\max} \sim \Delta t \sigma_K \rho_{at} |\mathcal{E}|^{2K}_{\max}$ is fixed by the pulse time scale Δt. This threshold is about 1.4×10^{13} W/cm^2 for pulse durations reduced to $t_p/10$. The peak electron density forms a plateau at $\rho^{\max} \sim 2 \times 10^{19}$ cm^{-3}, which remains coupled with the beam over one Rayleigh length, $z_0 = \pi w_0^2 n_0/\lambda_0 = 1.25$ mm. This coupling is robust, in the sense that the spatial size of the beam, decreased to $\sim w_0/3$ in the SF stage, is kept almost unchanged along this range. Figure 1(c) details the corresponding temporal profiles. MPI strongly shortens the pulse duration and only one sharp peak survives near the instant $t \sim -60$ fs. Dashed curves in Figs. 1(a) and 1(b) illustrate the modifications in the beam dynamics when dissipation is included. Whereas MPA lowers the peak intensity, a second focusing/defocusing cycle occurs, which enlarges the propagation domain to another Rayleigh length. Figure 1(d) reveals that the leading solitary pulse disperses more rapidly. This weakens plasma defocusing, which allows the emergence of a trailing peak pursuing the propagation on longer scales. Figures 1(e) and 1(f) describe the influence of the operators T and T^{-1} on the solitary pulse formed by MPI. Self-steepening occurs *after* MPI becomes active and does not prevent the formation of an electron plasma. Instead, it gives rise to a second high-intensity hump covering more than half of a Rayleigh length. A shock profile forms at $z \simeq 2.9$ mm [Fig. 1(g)], which results from the displacement of the front peak towards the rear of the pulse ($t > 0$). Addition of space-time focusing and MPA promotes comparable

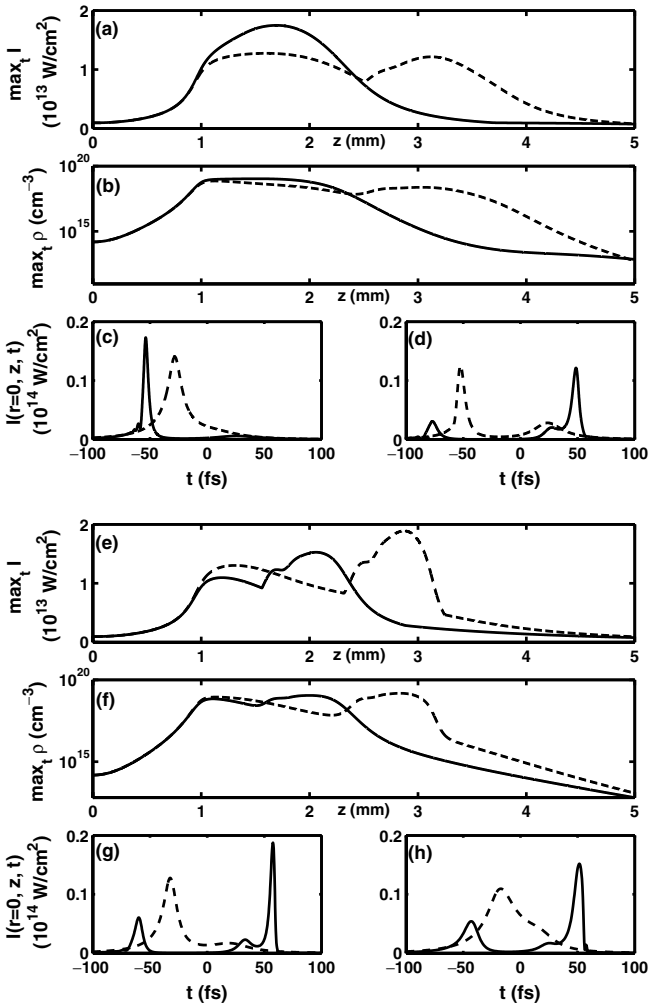

FIG. 1. Numerical simulations of 160 fs pulses with input powers $P_{\rm in} = 1.5P_{\rm cr}$ in silica glass. (a) On-axis ($r = 0$) peak intensity and (b) peak electron density without (solid curves) and with (dashed curves) MPA for $T = 1$. (c) Temporal profiles for MPI alone at $z = 1$ mm (dashed line) and $z = 1.8$ mm (solid line), displaying evidence of duration shortening. (d) Same with MPA at $z = 1.6$ mm (dashed line) and $z = 3.1$ mm (solid line). (e) Peak intensity and (f) electron density with no MPA and self-steepening alone (dashed curve) and with MPA and space-time focusing added (solid curve). Temporal profiles for these cases are shown in (g) for self-steepening only at $z = 1.45$ mm (dashed line) and $z = 2.9$ mm (solid line) and in (h) for the complete Eqs. (1) and (2) at $z = 1.2$ mm (dashed curve) and $z = 2.1$ mm (solid curve).

effects. The shock structure takes place at an earlier instant and is smoothed by MPA to some extent [Fig. 1(h)]. Up to a residual front portion, the resulting temporal profile mainly exhibits a single peak with duration still close to $t_p/10$, which propagates over $\sim z_0/2$.

To explain the above dynamics, we use the rescalings $r \to w_0 r$, $t \to t_p t$, $z \to 4z_0 z$, and $\mathcal{E} \to \sqrt{P_{cr}/4\pi w_0^2}\psi$ for notational convenience, which reduce Eqs. (1) and (2) to

$$i\partial_z\psi + \nabla_\perp^2\psi + (|\psi|^2 - \rho)\psi + \mathcal{F}(\psi) = 0, \qquad (3)$$

where the electron density ρ obeys $\partial_t\rho = \Gamma\,|\psi|^{2K}$ with $\Gamma = 1.22 \times 10^{-8}$. The function $\mathcal{F}(\psi) \simeq i\nu|\psi|^{2K-2}\psi + i(t_p\omega_0)^{-1}\partial_t[|\psi|^2\psi - \nabla_\perp^2\psi]$ follows from a straightforward Taylor expansion of the operator T^{-1} for an envelope frequency assumed to be smaller than ω_0. It mainly involves MPA with normalized coefficient $\nu = 3.24 \times 10^{-8}$ and deviations from the SVEA ($\omega_0 t_p = 324$). Variations in $i\partial_t(\rho\psi)/t_p\omega_0$ that act as higher-order MPA with relative weight $\sim\Gamma|\psi|^2_{\max}/t_p\omega_0\nu \leq 0.4$ have been discarded. Also, GVD with parameter $2z_0k''/t_p^2 = 4.6 \times 10^{-3}$ that measures the strength of dispersion relative to diffraction cannot split the pulse at power $P_{\rm in}/P_{\rm cr} = 1.5$ before MPI becomes active [9], and we henceforth ignore it.

Let us first discuss the case $\mathcal{F} = 0$. In the SF stage ($\rho = 0$), the beam envelope tends to collapse at a finite distance z_c, with the self-similar distribution [10]

$$\psi \to \frac{\sqrt{I(z,t)}}{R(z,t)}\phi(\xi)e^{i\int_0^z du/R^2(u,t) + iR_z R\xi^2/4}, \qquad (4)$$

where ϕ is the real solitary-wave solution of Eq. (3) with power equal to $P_c \equiv 11.7$, $\xi \equiv r/R(z,t)$, and $R(z,t) \sim [z_c(t) - z]^{1/2}$ denotes the wave radius that self-contracts as $z \to z_c$. Conservation of power $P = \int|\psi|^2 d\vec{r}$ then requires $I(t,z) = \alpha P_{\rm in}e^{-2t^2}/P_{\rm cr}$ where $\alpha = 4\pi/11.7$. For time-dependent pulses, the collapse distance z_c depends on the input beam parameters, and it must be reported to each cross section of the pulse ("time slice") as, e.g., $z_c(t) \simeq 0.16[\alpha P_{\rm in}/P_{\rm cr}e^{-2t^2} - 1]^{-0.635}$ for powers $P_{\rm in}/P_{\rm cr} < 2$ [11,12]. The central time slice focuses at the minimum distance $z_c(t=0)$, whereas $z_c(t)$ and $\dot{z}_c(t)$ reach infinity as $t \to \pm t^*$, where $t^* \equiv -[\ln\sqrt{\alpha P_{\rm in}/P_{\rm cr}}]^{1/2}$.

(i) *Plasma defocusing*: In the presence of ionization, the beam radius $R(z,t)$ evolves as follows (see [4]):

$$\frac{M}{4P_c}R^3R_{zz} = 1 - \alpha\frac{P_{\rm in}}{P_{\rm cr}}e^{-2t^2} - \frac{R^2}{2P_c}\int|\phi|^2\xi\partial_\xi\rho\, d\vec{\xi}, \qquad (5)$$

where $M \equiv \int\xi^2|\phi|^2 d\vec{\xi}$, while the last term refers to MPI with $\partial_\xi\rho \leq 0$. Because the time slices self-focus inside the narrow range $|t| < |t^*| < 1$ only, we assume that the temporal variations in the beam radius are relatively flat in the inner domain $t^2 \ll 1$ compared with e^{-2Kt^2}. The density function then behaves as

$$\rho(r,t,z) \simeq \sqrt{\frac{\pi}{8K}}\,\Gamma\!\left(\alpha\frac{P_{\rm in}}{P_{\rm cr}}\phi^2\right)^K\frac{{\rm Erf}(\sqrt{2K}t) + 1}{R^{2K}[z_c(t) - z]}. \qquad (6)$$

At positive times, the slices neighboring $t = 0$ are thus defocused by the density front becoming maximum in this range. In contrast, at negative times, the leading edge of the central slice continues to self-focus. The self-similarity assumption holds, which we can repeat at each time slice unaffected by the electron density. Plasma defocusing then develops step by step until a local equilibrium between SF and MPI is attained with $R_{zz} \to 0$. For $\Gamma \ll 1$ and $R(z,t)$ decreased to $R_0/3$ ($R_0 \simeq 0.81$ is defined by the incident beam profile), the fixed point of Eq. (5) is reached at the instant $t = t^* < 0$ only.

(ii) *MPA:* Multiphoton absorption introduces power dissipation as $\partial_z P = -2\nu\int|\psi|^{2K}d\vec{r}$. It acts at the moment when the pulse reaches its maximum intensity. MPA decreases the power in the above front peak and contributes to shorten its own self-guiding length as $I_z/I^K = -2\nu R^{2-2K}\int\phi^{2K}d\vec{\xi}/\int\phi^2 d\vec{\xi}$. By assuming an almost constant waist in self-trapped regimes and using $\phi(\xi) \sim \phi(0)e^{-R_0^2\xi^2}$, we find the normalized guiding length

$$\Delta z \simeq \frac{K}{K-1}\frac{\{[P(z_c)/P(z_f)]^{K-1} - 1\}}{2\nu|\psi|^{2K-2}_{\max}}, \qquad (7)$$

where z_f denotes the propagation distance from which, starting from the focus, the beam power goes below $P_{\rm cr}$. Note that the length (7) holds for radial distributions close to ϕ and thus for pulse powers near the critical value for SF only.

(iii) *Pulse steepening:* We first consider SF-dominated regimes, for which self-steepening is the main deviation from the SVEA. Ignoring diffraction, the field amplitude A ($\psi = Ae^{i\varphi}$) obeys the relation $A_z + 3A^2A_t/t_p\omega_0 = 0$, which admits the exact solution with implicit form: $A = F(t - 3zA^2/t_p\omega_0)$ [13]. For the "initial" distribution $|\psi|_0^2 = A_0^2{\rm sech}(\tau)$ where $\tau = (t - t^*)/T$ involves the front peak duration T, A and τ are linked by the relation

$$\tau = 3Q\frac{A^2}{A_0^2} + \cosh^{-1}\!\left[\frac{A_0^2}{A^2}\right], \qquad (8)$$

with $Q \equiv zA_0^2/t_p\omega_0 T$, so that a shock singularity ($\partial_t|\psi|^2 \to \infty$) arises as $Q \to 2/3$, i.e., at the distance $z_{\rm shock} = 2t_p\omega_0 T/3A_0^2$. When adding space-time focusing, transverse effects must be retained and the pulse power varies following the continuity relation,

$$\partial_z P = -\frac{\partial_t}{t_p\omega_0}\int\!\left(\frac{3}{2}\,|\psi|^4 + |\nabla_\perp\psi|^2\right)d\vec{r}, \qquad (9)$$

where the two integrals in the right-hand side tend to blow up in collapse regime [10]. Equation (9) then shows that the power in the pulse slices having $\partial_t|\psi|^2 < 0$ is strongly pushed to positive instants, so that space-time focusing also contributes to the formation of optical shocks. In terms of self-similar behaviors allowing for the replacement $\partial_t = -\dot{z}_c(t)\partial_z$, Eq. (9) can be written as $I_z \simeq (4/t_p\omega_0)\dot{z}_c\partial_z(I^2/R^2)$, which describes power displacement to positive times in the SF regime ($R_z < 0$) and recovers the result of [11] in the vicinity of $t = 0$.

Turning back to physical units, the previous behaviors can be summarized as follows: for the present parameters, the pulse is depleted slice after slice by MPI and converges to an equilibrium realized near the pulse cross section $t \simeq t^* t_p = -66$ fs having the critical power for SF. The resulting front peak is further damped by MPA over the guiding length $\Delta z \sim [(P_{\rm in}/P_{\rm cr})^{K-1} - 1]/\beta^{(K)}|\mathcal{E}|^{2K-2}_{\rm max} \simeq 1.2$ mm with $|\mathcal{E}|^2_{\rm max} \sim 10^{13}$ W/cm^2. As $|\mathcal{E}|^2$ decreases, ρ falls down significantly. This lets a second spike self-focus in the rear of the pulse over one more Rayleigh length. Pulse steepening, however, shortens this range to some extent. When modeling the front edge located at $z = 1.45$ mm in Fig. 1(g) by a sech function with duration $\sim\sqrt{\ln 2}t_p/5$, a shock emerges in the SF-dominated regime after the distance $z_{\rm shock} = 2\sqrt{\ln 2}t_p c/15n_2|\mathcal{E}|^2_{\rm max} \simeq 1.41$ mm. This shock hence occurs at $z \sim 2.9$ mm, while the time shift to the trail of the pulse is about 70 fs. These estimates are in good agreement with our numerical simulations.

Finally, Fig. 2 shows spectral broadening induced by the competition between Kerr and MPI (dashed line) and by mixing all nonlinearities from Eqs. (1) and (2) (solid line). Before pulse steepening occurs, variations in the nonlinear phase are given by $\varphi_z \sim |\psi|^2 - \rho$, where ρ depletes the back of the pulse. Consequently, the dominant modifications in the pulse spectrum is given by $\Delta\omega = -\varphi_t \sim \dot{z}_c/(z_c - z)$, which induces a strong redshifting with $\dot{z}_c \to -\infty$ as $t \to t^*$. Instead, when self-steepening occurs, phase variations lead to the spectral broadening $\Delta\omega/\omega_0 \simeq \{1 + [Q^2 - 2Q\sinh(\tau)]/\cosh^2(\tau)\}^{-1/2} - 1$ [13], which promotes a prominent blueshifting and weakens the MPI-redshifted pedestal. Both MPA and space-time focusing enhance this spectral dynamics, so that the resulting spectrum is mainly shifted to the blue side. At further propagation, the spectrum stabilizes in the wavelength domain shown in Fig. 2 (solid curve).

The above scenario holds for beam powers near critical ($P_{\rm in}/P_{\rm cr} < 2$). At higher powers, two peaks instead rapidly emerge in regions in time where the beam power is still above critical [5]. Such temporal distortions can be confronted with the generic self-compression of 200-fs pulses to shorter durations experimentally reported in [14]. In a Comment [15], arguments raised the possibility of creating free electrons at beam intensities close to 10^{13}–10^{14} W/cm^2, for which ionization can extract the outmost bound electrons of neutral atoms over the pulse time scale and may contribute to self-compression. Our analysis shows that, at these intensities, plasma generation is indeed able to cause an efficient pulse compression.

In summary, we have shown that ultrashort solitary pulses resulting from the balance between MPI and SF form in silica samples at input powers moderately above critical. Although space-time focusing and self-steepening modify this property by inducing shock dynamics, they can sustain the propagation of very short pulses while keeping MPI active. In this power domain, a propagation range close to the Rayleigh length covered by intense solitary pulses with durations compressed to a few fs is thus physically accessible, which could have important applications in pulse shortening techniques.

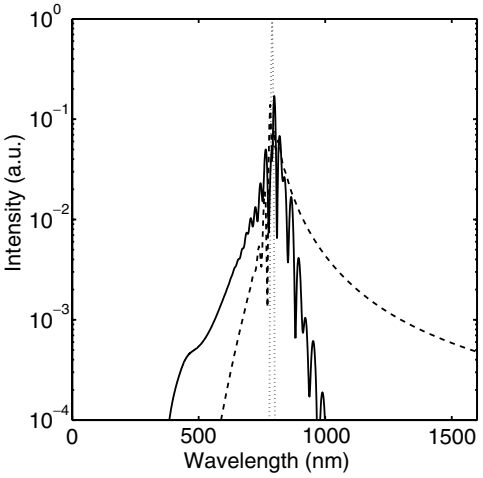

FIG. 2. Power spectra of 160-fs pulses with $P_{\rm in}/P_{\rm cr} = 1.5$ in silica for the input beam (dotted line), for a pulse with MPI alone at $z = 1.8$ mm (dashed line), and for the same pulse described by Eqs. (1) and (2) at $z = 2.1$ mm (solid line).

The authors thank Dr. A. Couairon for assistance in the numerical computations.

[1] A. Braun *et al.*, Opt. Lett. **20**, 73 (1995); E. T. J. Nibbering *et al.*, Opt. Lett. **21**, 62 (1996); H. R. Lange *et al.*, Opt. Lett. **23**, 120 (1998); B. LaFontaine *et al.*, Phys. Plasmas **6**, 1615 (1999); L. Wöste *et al.*, Laser Optoelektron. **29**, 51 (1997); A. Couairon *et al.*, J. Opt. Soc. Am. B **19**, 1117 (2002).
[2] M. Mlejnek, E. M. Wright, and J. V. Moloney, Opt. Lett. **23**, 382 (1998).
[3] L. Bergé and A. Couairon, Phys. Plasmas **7**, 210 (2000).
[4] L. Bergé and A. Couairon, Phys. Rev. Lett. **86**, 1003 (2001).
[5] S. Tzortzakis *et al.*, Phys. Rev. Lett. **87**, 213902 (2001).
[6] S. Henz and J. Herrmann, Phys. Rev. A **59**, 2528 (1999).
[7] A. L. Gaeta, Phys. Rev. Lett. **84**, 3582 (2000).
[8] T. Brabec and F. Krausz, Phys. Rev. Lett. **78**, 3282 (1997).
[9] G. G. Luther, J. V. Moloney, A. C. Newell, and E. M. Wright, Opt. Lett. **19**, 862 (1994).
[10] L. Bergé, Phys. Rep. **303**, 259 (1998).
[11] G. Fibich and G. Papanicolaou, Opt. Lett. **22**, 1379 (1997); SIAM J. Appl. Math. **60**, 183 (1999).
[12] A. Brodeur *et al.*, Opt. Lett. **22**, 304 (1997).
[13] D. Anderson and M. Lisak, Phys. Rev. A **27**, 1393 (1983); G. Yang and Y. R. Shen, Opt. Lett. **9**, 510 (1984).
[14] I. G. Koprinkov *et al.*, Phys. Rev. Lett. **84**, 3847 (2000); Phys. Rev. Lett. **87**, 229402 (2001).
[15] A. L. Gaeta and F. Wise, Phys. Rev. Lett. **87**, 229401 (2001).